

OVERSHOOTING TOP OF CONVECTIVE CLOUD IN EXTREME WEATHER EVENTS OVER JAVA REGION BASED ON VISUAL IDENTIFICATION OF HIMAWARI 8 IMAGERY

Bony Septian Pandjaitan ^{1,2}, Akhmad Faqih ¹, Furqon Alfahmi ^{2*}, Perdinan ¹

¹Department of Geophysics and Meteorology, IPB University, Bogor, 16680, Indonesia

²Agency for Meteorology, Climatology, and Geophysics, Jakarta, 10610, Indonesia

*E-mail: furqon.alfahmi@bmk.go.id

Article submitted: November 23, 2022

Article revised: May 7, 2023

Article accepted: July 27, 2023

ABSTRACT

Overshooting top (OT) in convective clouds is an essential feature in extreme weather nowcasting performed by weather forecasters to represent the core location of the severe region of the convective cloud. In addition, we can estimate the location of extreme weather events by utilising OT climatology. Unfortunately, it cannot be realised in tropical Indonesia, especially on Java Island at present, because there still needs to be more research on the presence of OT in extreme weather events. This research aims to study the presence of OT in extreme weather events on Java Island using extreme weather reports and the Himawari 8 satellite data. We detect the presence or absence of OT patterns at the location of the extreme weather event with Visual identification by using a visible channel (0.64 μm) with a spatial resolution of 500 m and sandwich products. We found that about 87% of extreme weather occurred accompanied by the appearance of OT patterns from convective clouds. A parallax effect of Himawari 8 caused the detected OT location in the southwest direction of the actual location. Extreme weather events accompanied by the OT feature of convective clouds most often occur in the transitional period of the rainy to dry season (MAM) and the rainy season (DJF). Meanwhile, extreme weather events rarely occur during the dry season (JJA). Extreme weather events accompanied by OT often occur from midday to late afternoon. OT in this study has a diameter between 2-15 km during extreme weather events. A time lag between the appearance of OT and extreme weather events in Java Island gives us opportunities for approximating and nowcasting the extreme weather events.

Keywords: convective cloud, extreme weather, Himawari 8 satellite, overshooting top.

1. Introduction

The overshooting top (OT) is the top feature of the cumulonimbus cloud, which has a dome-like 'protrusion'. This region has a reasonably strong updraft on the internal part that penetrates through its equilibrium level (EL) or level of neutral buoyancy (LNB) and can also penetrate the tropopause up to the lower stratosphere [1].

Several previous studies outside the Territory of Indonesia mentioned the importance of OT in nowcasting because OT represents the core location of the severe region in the convective cloud. A convective cloud with OT has a strong and continuous updraft inside it. It is the reason that causes convective clouds with OT features can produce extreme weather, such as heavy rain, strong winds, large hail, and tornadoes [2]–[9].

The strong linkage between OT locations and extreme weather locations shows us that identifying the OT regions can increase the nowcasting confidence of a convective cloud that can produce extreme weather, especially if there is no ground-based weather radar [2]. In addition, the strong linkage between OT

locations and extreme weather locations has led to OT studies in subtropical regions already utilising OT feature climatology from satellite data to estimate extreme weather event locations for Europe, America, and Australia [2], [10]–[15].

It cannot be realised in the tropical regions of Indonesia, especially on Java Island, because there are still little numbers of research on the presence of OT in extreme weather events [16]. In addition, some of these previous studies did not investigate OT as the main subject of their discussion and only examined a case of extreme weather events [17]–[19]. Therefore, as an initial stage to estimate and nowcast the extreme weather events based on the presence of OT, we aim to study the presence of OT in extreme weather events in Indonesian territory, both in terms of their relationship, as well as their spatial and temporal distribution. Initially, the study was carried out based on cases of extreme weather on the island of Java based on visual identification of OT using a higher resolution visible channel of the Himawari 8 satellite.



Figure 1. The physical form of the overshooting top (OT) on convective clouds inside the red polygon (source: <https://pin.it/4JBtL1k>)

2. Methods

The location of this study covers the mainland area of Java Island with a data period of 4 years (January 2018 – December 2021). Figure 2 gives information about the focus area of this study. This study used several data, such as extreme weather events reports and Himawari 8 Satellite data.

We obtained data on reports of extreme weather events from the Sub-Division for Weather Early Warning of the Indonesia Agency for Meteorology, Climatology, and Geophysics. The types of extreme weather used in research include heavy rain, strong winds, ‘puting beliung’ (smaller scale tornado), and hail. The types of extreme weather we use follow the criteria for extreme weather events from the Agency for Meteorology, Climatology and Geophysics of the Republic of Indonesia [20], [21]. However, when filtering extreme weather report data, we selected it based on reports of hail events followed by other types of extreme weather, such as heavy rain, strong winds, and tornadoes.

We used Himawari 8 satellite data with a wavelength channel of $0.64 \mu\text{m}$; and $10.4 \mu\text{m}$. We also obtained Himawari 8 Satellite data from JMA (Japan Meteorological Agency), which is received every 10 minutes by the BMKG Weather Satellite Imagery Management Sub-Division through the Himawari-Cloud network. The visible channel ($0.64 \mu\text{m}$) of Himawari satellite data used in the study has a spatial resolution of 500 meters, while the IR channel data ($10.4 \mu\text{m}$) has a spatial resolution of 2 km. All satellite channels used in the study have a temporal resolution every 10 minutes [22].

In this study, after collecting all the data, the selected extreme weather data screening was carried out by choosing hail events that were accompanied or not accompanied by other types of extreme weather. This filtering was accompanied by the event region's information attributes and the event's time in UTC units (H-7 hours from the local time).

Furthermore, based on the coordinates of the location and time of the selected extreme weather event, visual identification of the presence of OT around the location was carried out using a visible channel ($0.64 \mu\text{m}$) according to the definition of the OT pattern. The visible channel has a spatial resolution of 500 m, the highest spatial resolution channel in the Himawari 8 Satellite [22]. Several previous studies also detected the presence of OT visually using visible channel data ($0.64 \mu\text{m}$). However, they intend to construct OT databases as validation data for objective methods in detecting OT in their research [8], [23], [24]. We also used the sandwich product, as seen in Figure 3d, to strengthen the OT identification results, a merge (blend) between the visible channel ($0.64 \mu\text{m}$) and the IR channel ($10.4 \mu\text{m}$), allowing observation of all of these features simultaneously, in one single product [25].

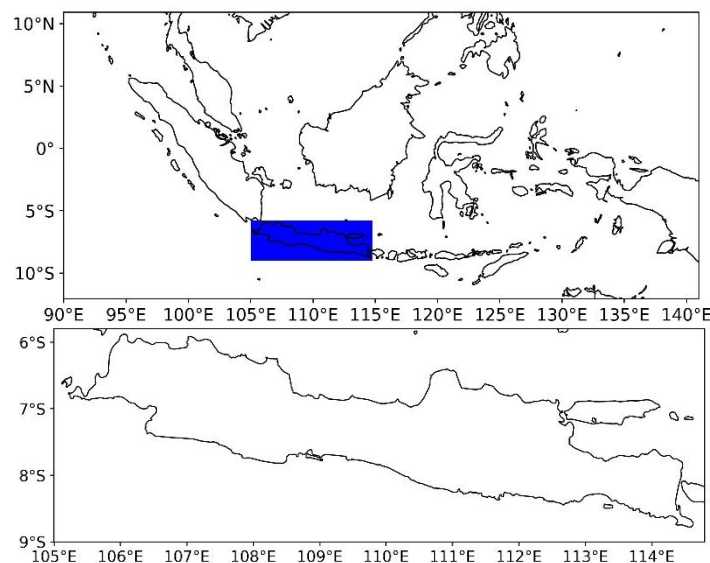


Figure 2. The research area covers the mainland of Java Island.

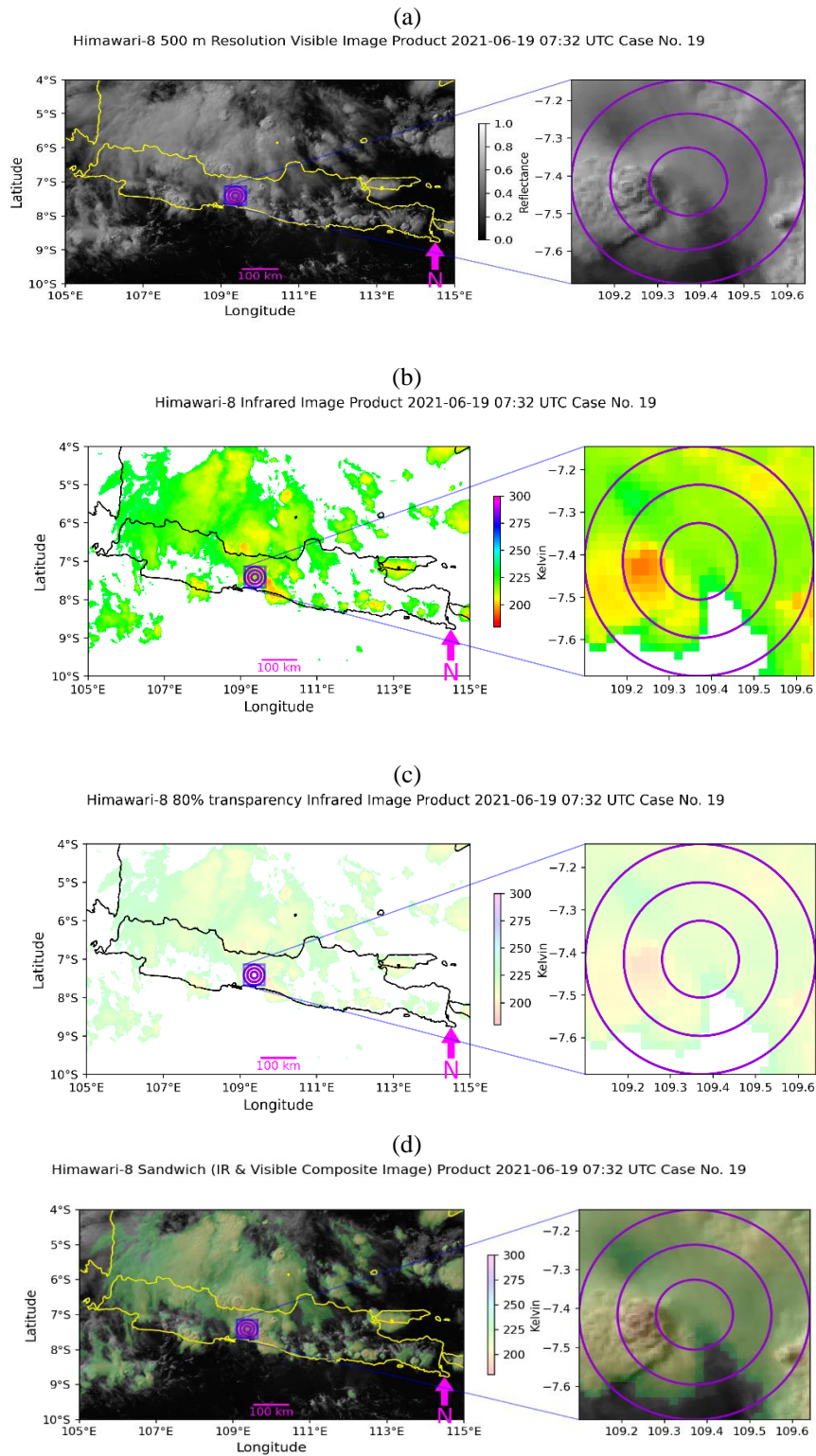


Figure 3. Left/right side of each image shows the location of overshooting top and extreme weather event (midpoint of the purple circle) in the Java area / specific area on June 10th, 2021, at 07:32 UTC (14:32 LT) for: (a) 500 m resolution visible image, (b) infrared enhanced image, (c) infrared enhanced image with 80% transparency, and (d) sandwich image. Each of the purple circles has a distance interval of a 10 km radius.

(a)

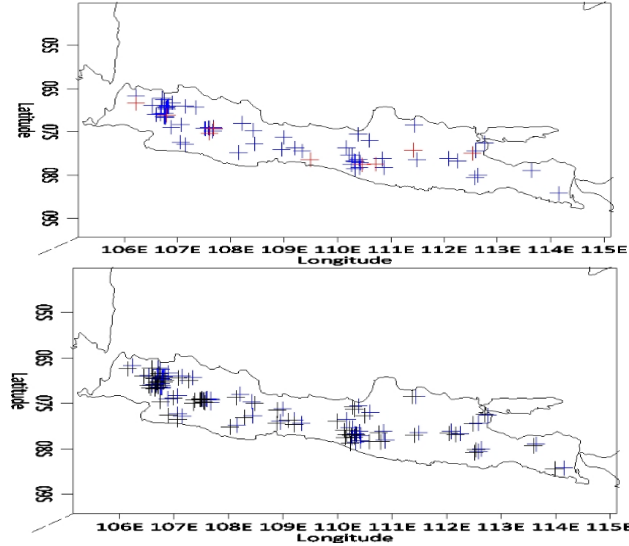


Figure 4. The accumulation during the 2018-2021 period for a) the location of extreme weather events which are accompanied and not accompanied by OT patterns, and b) the location of extreme weather events which are accompanied by OT patterns along with the location of the overshooting top (OT). The blue '+' sign indicates the location of the extreme weather event accompanied by the OT pattern, while the red '+' sign indicates the location of the extreme weather event where there is no OT pattern. The black '+' sign indicates the nearest OT location without parallax correction from the extreme weather location.

The sandwich image product consists of two layers. The bottom layer, as seen in Figure 3a, is a black-and-white visible channel image showing the reflectance values of the solar channels and the texture of the clouds. The top layer, as seen in Figure 3b, is a colour-enhanced IR window image showing details of the brightness-temperature field. Then, we set the colour-enhanced IR image with 80% transparency, as seen in Figure 3c. Finally, we merged the visible channel image in Figure 3a as the bottom layer and the colour-enhanced IR image with 80% transparency in Figure 3c as the top layer to produce the sandwich image in Figure 3d.

After obtaining OT data on the location and time of the selected extreme weather event, we recorded the coordinates and time of the nearest OT appearance from the location of extreme weather events. We realised it to measure the distance between the OT location and the selected extreme weather events location, which is affected by the parallax effect of the Himawari 8 satellite. In addition, we also determine the time interval between the time of OT events and the time of selected extreme weather events.

We also calculate the parallax correction of OT location and then correct the location of OT. An object at altitude h_{cloud} observed from a satellite at altitude h_{sat} above the centre of the earth is actually at a slightly different position than the satellite recorded position, so parallax correction of the altitude information (e.g. cloud top height) is required.

We used some input parameters for correcting the parallax effect, such as satellite height above the earth's centre in km (h_{sat}), the latitude of the subsatellite point φ_{sat} , the longitude of the subsatellite point (λ_{sat}), the height of the observed cloud in km (h_{cloud}), the assigned latitude of the object (φ_{cloud}), and assigned longitude of the object (λ_{cloud}). The output parameter of parallax correction calculation consists of the parallax corrected latitude of the object ($\varphi_{cloud,corr}$) and parallax corrected longitude of the object ($\lambda_{cloud,corr}$). We also used static data, such as earth radius, equator in km (R_{equ}), earth radius pole in km (R_{pole}), and mean earth radius in km ($R_{mean} = 0.5 (R_{equ} + R_{pole})$, radius ratio ($R_{ratio} = R_{equ} / R_{pole}$).

Calculating the parallax correction begins with express satellite position in cartesian coordinates.

$$x_{sat} = h_{sat} \cos(\varphi_{sat, geod}) \sin(\lambda_{sat}) \quad (1)$$

$$y_{sat} = h_{sat} \sin(\lambda_{sat}) \quad (2)$$

$$z_{sat} = h_{sat} \cos(\varphi_{sat, geod}) \cos(\lambda_{sat}) \quad (3)$$

Where $\varphi_{sat, geod}$ is the geodetic latitude of the subsatellite point, defined as:

$$\varphi_{sat, geod} = \arctan[\tan(\varphi_{sat}) R_{ratio}^2] \quad (4)$$

The next step is expressing the surface position in cartesian coordinates.

$$x_{cloud} = R_{local} \cos(\varphi_{cloud, geod}) \sin(\lambda_{cloud}) \quad (5)$$

$$y_{cloud} = R_{local} \sin(\lambda_{cloud}) \quad (6)$$

$$z_{cloud} = R_{local} \cos(\varphi_{cloud, geod}) \cos(\lambda_{cloud}) \quad (7)$$

Where R_{local} is the earth's radius, and $\varphi_{cloud, geod}$ is the geodetic latitude, according to

$$R_{local} = \frac{R_{eq}}{\sqrt{\cos^2(\varphi_{cloudgeod}) + R_{ratio}^2 \sin^2(\varphi_{cloudgeod})}} \quad (9)$$

$$\varphi_{cloudgeod} = \arctan[\tan(\varphi_{cloud})R_{ratio}^2]$$

The next step is computing the local ratio of earth radii, corrected for cloud top height (squared).

$$R_{ratio,local} = \left(\frac{R_{equ} + h_{cloud}}{R_{pole} + h_{cloud}} \right)^2 \quad (10)$$

A further step is computing the difference vector between the satellite and the cloud position

$$x_{diff} = x_{sat} - x_{cloud} \quad (11)$$

$$y_{diff} = y_{sat} - y_{cloud} \quad (12)$$

$$z_{diff} = z_{sat} - z_{cloud} \quad (13)$$

Then, compute the correction for the line of sight at the cloud top height h_{cloud} .

$$c = \frac{\sqrt{e^2 - 4e_1e_3 - e_2}}{2e_1} \quad (15)$$

with

$$e_1 = x_{diff}^2 - R_{ratio,local} y_{diff}^2 + z_{diff}^2 \quad (16)$$

$$e_2 = 2(x_{cloud}x_{diff} + R_{ratio,local}y_{cloud}y_{diff} + z_{cloud}z_{diff}) \quad (17)$$

$$e_3 = x_{cloud}^2 - R_{ratio,local}y_{cloud}^2 + z_{cloud}^2 - (R_{equ} + h_{cloud})^2 \quad (18)$$

Then, we apply correction to the cartesian coordinates of the cloud position.

$$x_{corr} = x_{cloud} - cx_{diff} \quad (19)$$

$$y_{corr} = y_{cloud} - cy_{diff} \quad (20)$$

$$z_{corr} = z_{cloud} - cz_{diff} \quad (21)$$

x_{corr} , y_{corr} and z_{corr} are now the cartesian coordinates of the parallax corrected location. Finally, we convert corrected cartesian coordinates back to latitude and longitude.

$$\varphi_{cloudcorr} = \arctan \left[\frac{\tan \left(\arctan \frac{y_{corr}}{\sqrt{x_{corr}^2 + z_{corr}^2}} \right)}{R_{ratio}^2} \right] \quad (22)$$

$$\tan(\lambda_{cloud,corr}) = \frac{x_{corr}}{z_{corr}} \quad (23)$$

The corrected longitude $\lambda_{cloud,corr}$ can be achieved by the computer program ATAN2 function, which is given two arguments:

$$\lambda_{cloud,corr} = ATAN2(x_{corr}, y_{corr}) \quad (24)$$

Furthermore, we calculated a percentage of OT occurrences when extreme weather occurred. The detected OT from visible channels and sandwich products around the location of the weather events were used to see the percentage of OT occurrences during selected extreme weather events. We realised it to find out the relationship between the appearances

of OT when a selected extreme weather event occurred. The appearance of OT convective clouds during extreme weather indicated that convective clouds with this OT can produce extreme weather.

$$\% \text{OTExtWx} = \frac{\sum \text{ExtWxOT}}{\sum \text{ExtWx}} \times 100\% \quad (25)$$

Where % OTExtWx is percentage of OT when a selected extreme weather event occurred, ExtWxOT is selected extreme weather with OT, and ExtWx is selected extreme weather.

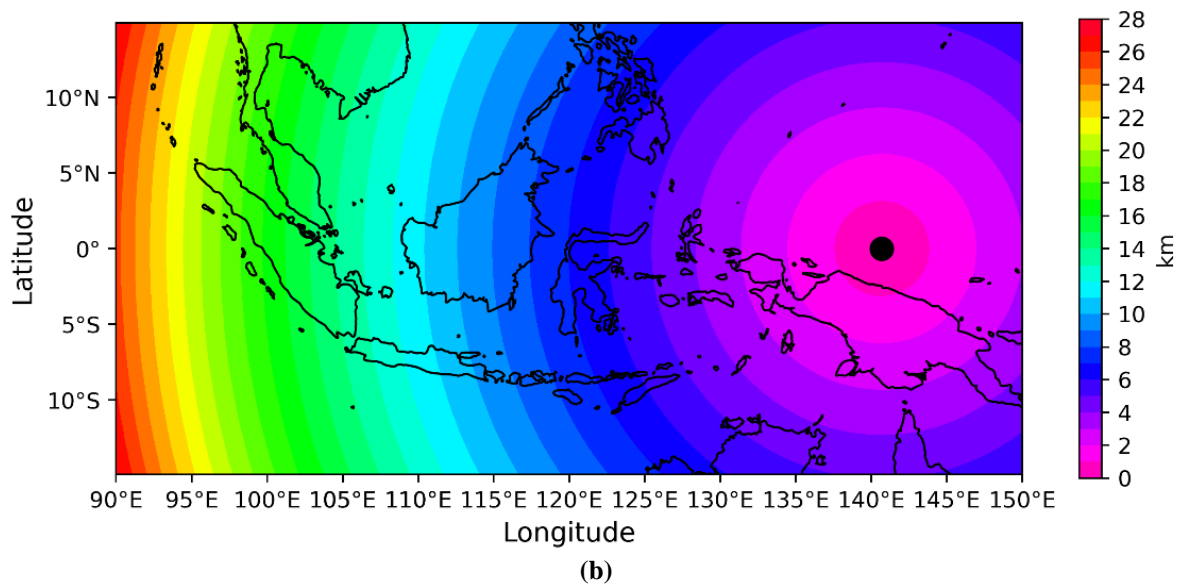
3. Result and Discussion

Based on the data of extreme weather events report and image processing of visible channels of Himawari 8 satellite in the 2018-2021 period, we can see the spatial distribution of extreme weather event locations and Overshooting Top (OT) locations in Figure 4. The spatial distribution of the extreme weather events during 2018-2021, as seen in Figure 4a, was in the western, central, and eastern parts of Java Island, where there were mostly OTs at every extreme weather event. There were only very few cases where OT did not appear during extreme weather events in the western, central, and eastern parts of Java Island.

Based on Figure 4b, the OT pattern that appeared during extreme weather from 2018 to 2021 differs from the extreme weather locations. There was a location shifting in each occurrence of OT during extreme weather. It means the OT was not at the actual coordinates.

Based on Figure 5b, the distance between the location of the convective cloud OT pattern and the location of extreme weather has a range of values between 5-22 km with lower and upper quartile values of about 11 and 15 km. It happened due to a location shift due to the parallax of the Himawari 8 satellite, where the OT location detected from the Himawari 8 satellite shifted from the actual location. It is consistent with the information in Figure 5a regarding the results of the parallax correction calculation based on the cloud top height of 15 km. This match explains the reason for the difference in the location of the convective cloud OT pattern with extreme weather locations on Java Island, where the OT has a reasonably high height. The range of OT shift values due to this parallax will be greater than those in Figure 5a if the cloud top or OT height of more than 15 km and vice versa. Therefore, based on the distance between the OT location to the extreme weather location in Figure 5a with the calculation of Himawari 8 parallax correction to the cloud top height of 15 km in Figure 5b indicates that the OT detected in this study had a height of ≥ 15 km.

(a)



(b) Box Plot of Distance between OT Locations and Extreme Weather Period 2018 - 2021

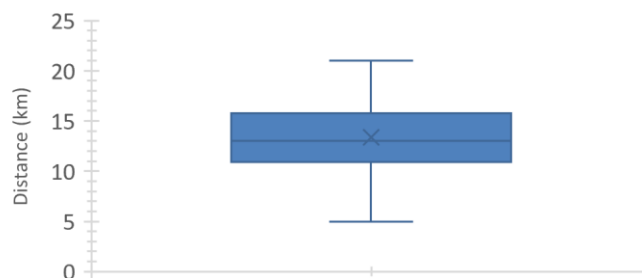


Figure 5 a) Shifting (in km) or parallax correction of Himawari 8 Satellite based on cloud top height of 15 km for the entire Territory of Indonesia. The "●" sign indicates the location of the Himawari 8 Satellite. b) Box plot for the distance between OT location without parallax correction and extreme weather location for the 2018-2021 period in Java Island.

In addition, as explained earlier, the difference in location between extreme weather and OT can be further away due to the parallax effect that naturally occurs in observations from satellites orbiting above the earth. The distance of the difference in location between extreme weather and OT in this study is still smaller than the results of several previous studies in the subtropical region. For example, the study of Bedka [2] used extreme weather report data in the form of hail from the European Severe Weather Database (ESWD) to investigate OT. The difference in location between the OT and the hail events is 25 km for reports with a confidence interval of ± 15 minutes and a maximum of 75 km for reports with a confidence interval of ± 60 minutes (1 hour). Meanwhile, Punge et al. [26] 's study stated that the location difference between the extreme weather and OT is in an area of 1000 km².

We can see the spatial distribution of extreme weather event locations accompanied by or not accompanied by OT locations each year in the 2018-2021 period in

Figure 6. Based on the information in each year of the 2018-2021 period indicates that every extreme weather event accompanied by an OT has an OT location which generally shifts to the southwest of the OT's actual location and each extreme weather event location. It happened due to the satellite parallax effect, where Himawari 8 has an orbital location in the northeast direction of Java Island, as in Figure 5a. Based on Figure 6, after correcting the parallax effect based on the cloud top height of 15 km, the location of overshooting tops is generally near the extreme weather events location.

Information on temporal extreme weather events in Java during the 2018-2021 period can be seen in Figure 7. Extreme weather events mainly occurred in March, April, and December. Those Months are the transitional season of the rainy to dry season (MAM) and the rainy season (DJF). Meanwhile, infrequent extreme weather events occurred around July and August (JJA), correlating to the dry season.

(a)

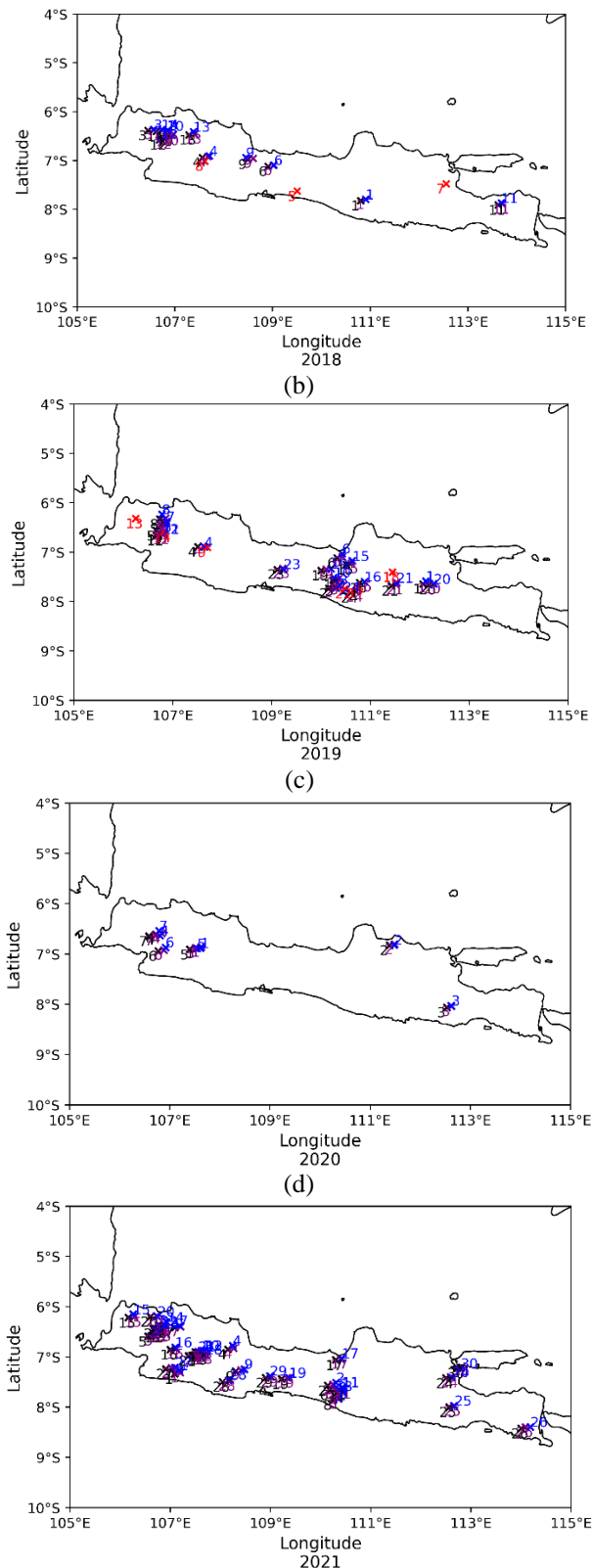


Figure 6 Distribution map of extreme weather events and overshooting top (OT) locations detected in Java Island for the following periods: a) 2018, b) 2019, c) 2020, and d) 2021. The numbers indicate the sequence number of extreme weather events in each period. Blue X numbers and signs indicate the location of extreme weather events accompanied by OT patterns. In contrast, red X numbers and signs indicate the location of extreme weather events with no OT pattern. Black X numbers and signs indicate the nearest OT location without parallax correction of the extreme weather event. Purple X numbers and signs indicate the nearest OT location with parallax correction of the extreme weather event.

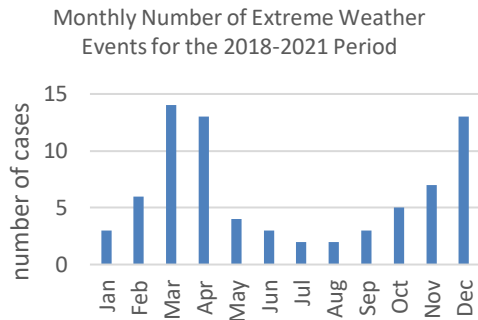


Figure 7 The number of extreme weather events for the 2018-2021 period in Java Island for every month

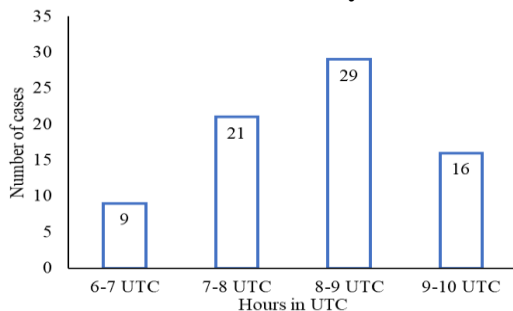


Figure 8 Temporal distribution of extreme weather events for the 2018-2021 period on Java Island

The extreme weather events for the 2018-2021 period occurred from midday to late afternoon, as seen in Figure 8, where 8 – 9 UTC or 15-16 LT is the period for the most frequent occurrence of extreme weather. The period of this event is similar to the period of the diurnal convective cycle when the convective process due to solar heating with sufficient air humidity will form convective clouds during the day to evening [27]. Convective clouds from afternoon to evening today could potentially result in extreme weather.

Information on the presence of OT during extreme weather events based on the annual accumulation of the 2018-2021 period, as in Figure 9a, shows that OT accompanies most or about 87% of extreme weather events. It also bears a resemblance to some previous studies conducted in other regions. Research by Bedka et al. [28] and Dworak et al. [5] in the United States region showed that 57% and 42% of convective clouds that have OT features produce extreme weather, respectively, while for the European Region, about 47% of convective clouds that have OT features are found near regions where extreme weather events [2]. It proves that the OT is a pattern or feature of convective clouds closely related to extreme weather events for the Java Island region in this study and other regions in the previous study. Figure 9b shows that during 2018 in Java Island, around 79% of extreme weather events were accompanied by OT patterns, and in 2019 there were around 71% of extreme weather events accompanied

by OT patterns. Meanwhile, in 2020 and 2021, all extreme weather events are accompanied by OT patterns. In addition, in 2018 and 2019, only about 14% and 21% of extreme weather events were not accompanied by OT patterns. The details are cases 5 and 7 for 2018 and cases 9, 13, 14, 17, and 19 for 2019, where the case numbers can be seen in Figure 6.

The occurrences of extreme weather not accompanied by OT patterns can be caused by other factors beyond the limitations of this study. Another thing that may be a factor in OT's undetectability during extreme weather events based on previous studies, generally in subtropical regions, is that OT has a life cycle variation of 5 - 20 minutes [10]. In other studies, it can even reach less than 5 minutes when using satellites with a super rapid scan observation mode every 1 minute on the GOES Satellite [5]. Consequently, when the Himawari 8 scanning time arrives, The OT has yet to form. However, after Himawari 8 has finished scanning, the OT is formed and has become extinct before the next Himawari 8 scanning time or hour, which every 10 minutes start again. The faster or higher the temporal resolution of the satellite, the more likely it is that the number of OT that the satellite can detect [29].

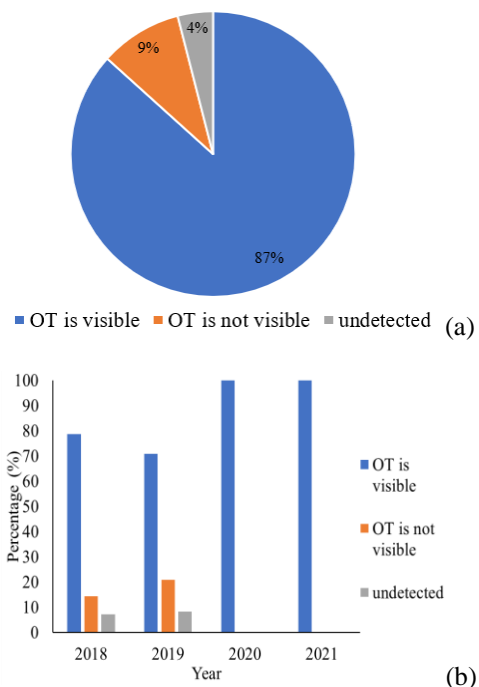


Figure 9 Percentage of the occurrences of OT patterns during extreme weather events for the 2018-2021 period in Java Island for a) accumulation of 2018-2021 and b) every year (starting from 2018 at the inner circle to 2021 at the outer circle).

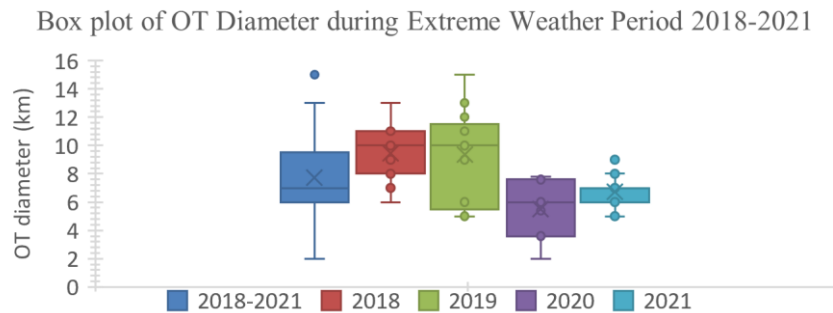


Figure 10 Box plot of OT diameter during extreme weather events for the 2018-2021 period in Java Island

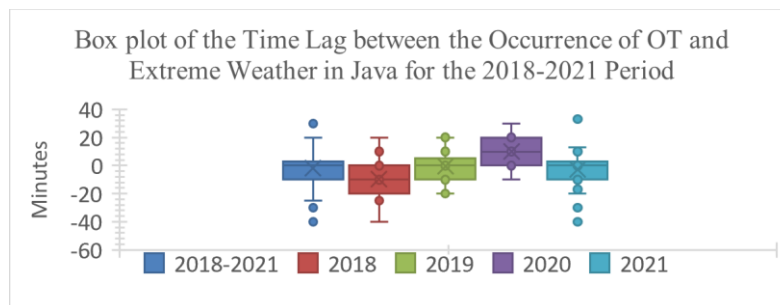


Figure 11 Box plots the time interval between the appearance of OT and extreme weather events in the 2018-2021 period on Java Island.

In addition, in 2018 and 2019, about 7% and 8% of extreme weather events could not be detected by the presence or absence of OT patterns. The details are case number 8 in 2018, as in Figure 5a, and case numbers 18 and 22 of 2019, as in Figure 5b. It is due to the time of extreme weather events that occur in the afternoon before evening or around 10 UTC (17:00 WIB). At that time, the sun's position is already low, reducing the sunlight that reaches the surface. Due to the ability of the Himawari 8 visible channel to be reduced in detecting cloud objects, including OT, it cannot be determined whether there is OT during extreme weather events.

Figure 10 shows that the overshooting top (OT) has a 2-15 km diameter during extreme weather events from 2018- 2021 on Java Island. Some previous studies mentioned that the size or diameter of OT can reach 15 km [4], [30], while other studies mention up to 20 km [5], [8], [31]. In addition, there is a relationship between size or diameter and the duration or period of OT events. The more extensive OT diameter generates a longer duration or period of OT occurrences [32]. Previous research has shown that long-lasting OT usually consists of many OT individual towers with a much smaller diameter (1 km) and a shorter period of about 1-2 minutes [30]. The time interval for OT with extreme weather events on Java Island during 2018-2021 is about 40 minutes before and after extreme weather events, as seen in Figure 11. The results of this study are similar to the result in the United States region, which shows that

about 85% of convective clouds containing OT features have an interval of about 18 minutes before extreme weather occurs [28]. It is also supported by the research of Dworak et al. [5] in the United States, which states that 75% of OT is detected before extreme weather occurs. It proves that the OT feature of convective clouds can be used as an approximation or nowcasting for the appearance of extreme weather.

4. Conclusion

Most extreme weather events are accompanied by OT patterns from convective clouds, where OT patterns accompany about 87% of extreme weather events. It proves that the OT pattern is a pattern or feature of convective clouds closely related to extreme weather events in the Java Island region. This research shows that not all OT in extreme weather events can be detected. The reason is that OT has a rapid life cycle variation of 5-20 minutes, so more time is needed for OT to be observed by the Himawari 8 satellite, which has an observation frequency every 10 minutes. The difference in location between OT location coordinates and extreme weather location coordinates is due to a location shift from the Himawari 8 satellite parallax with a shift to the southwest of each extreme weather event location. Extreme weather events accompanied by the OT feature of convective clouds most often occur in the transitional season of the rainy to dry season (MAM) and the rainy season (DJF). Meanwhile, extreme weather events rarely occur during the dry season (JJA).

The extreme weather events accompanied by the OT feature of convective clouds often occurs from midday to late afternoon. These studies' overshooting tops (OT) have a diameter size of 2 - 15 km during extreme weather events. A time interval between the appearance of OT and extreme weather events in Java Island shows that the OT feature of convective clouds can be used as a proxy and nowcasting for the appearance of extreme weather.

The results of this study prove that the presence of OT is closely related to extreme weather events on the island of Java, which is part of the territory of Indonesia. It can be a reference for similar research in other regions of Indonesia. In addition, the results of this study with visible channel data with a resolution of 500 m can be used as training and validator data to develop an objective detection method for OT in the Indonesian Territory, especially Java Island, using data from various infrared channels from the Himawari 8 satellite which are available both day time and night time.

Acknowledgement

This research received support from the Agency for Meteorological Climatology and Geophysics for acquiring Himawari 8 Satellite data and the report of extreme weather events. The first author thanked the Education and Training Center of the Meteorological Climatology and Geophysics Agency for providing scholarships in the Applied Climatology master's program at IPB University and funding for this research.

References

- [1] Glickman, "Glossary of Meteorology,." 2000.
- [2] K. M. Bedka, "Overshooting cloud top detections using MSG SEVIRI Infrared brightness temperatures and their relationship to severe weather over Europe," *Atmospheric Research*, vol. 99, no. 2, pp. 175–189, Feb. 2011, doi: 10.1016/j.atmosres.2010.10.001.
- [3] H. B. Bluestein, D. T. Lindsey, D. Bikos, D. W. Reif, and Z. B. Wienhoff, "The Relationship between Overshooting Tops in a Tornadic Supercell and Its Radar-Observed Evolution," *Monthly Weather Review*, vol. 147, no. 11, pp. 4151–4176, Nov. 2019, doi: 10.1175/MWR-D-19-0159.1.
- [4] J. C. Brunner, S. A. Ackerman, A. S. Bachmeier, and R. M. Rabin, "A Quantitative Analysis of the Enhanced-V Feature in Relation to Severe Weather," *Weather and Forecasting*, vol. 22, no. 4, pp. 853–872, Aug. 2007, doi: 10.1175/WAF1022.1.
- [5] R. Dworak, K. Bedka, J. Brunner, and W. Feltz, "Comparison between GOES-12 Overshooting-Top Detections, WSR-88D Radar Reflectivity, and Severe Storm Reports," *Weather and Forecasting*, vol. 27, no. 3, pp. 684–699, Jun. 2012, doi: 10.1175/WAF-D-11-00070.1.
- [6] F. Li and F. Yu, "MTSAT-1R satellite-based overshooting top detection and the relationship to precipitation intensity," presented at the SPIE Asia Pacific Remote Sensing, E. Im, S. Yang, and P. Zhang, Eds., Beijing, China, Nov. 2014, p. 92590E. doi: 10.1117/12.2068678.
- [7] G. R. Marion, R. J. Trapp, and S. W. Nesbitt, "Using Overshooting Top Area to Discriminate Potential for Large, Intense Tornadoes," *Geophys. Res. Lett.*, vol. 46, no. 21, pp. 12520–12526, Nov. 2019, doi: 10.1029/2019GL084099.
- [8] P. Mikuš and N. Strelec Mahović, "Satellite-based overshooting top detection methods and an analysis of correlated weather conditions," *Atmospheric Research*, vol. 123, pp. 268–280, Apr. 2013, doi: 10.1016/j.atmosres.2012.09.001.
- [9] P. Mikuš Jurković, N. S. Mahović, and D. Počakal, "Lightning, overshooting top and hail characteristics for strong convective storms in Central Europe," *Atmospheric Research*, vol. 161–162, pp. 153–168, Jul. 2015, doi: 10.1016/j.atmosres.2015.03.020.
- [10] K. Bedka, J. Brunner, R. Dworak, W. Feltz, J. Otkin, and T. Greenwald, "Objective Satellite-Based Detection of Overshooting Tops Using Infrared Window Channel Brightness Temperature Gradients," *Journal of Applied Meteorology and Climatology*, vol. 49, no. 2, pp. 181–202, Feb. 2010, doi: 10.1175/2009JAMC2286.1.
- [11] S. R. Proud, "Analysis of overshooting top detections by Meteosat Second Generation: a 5-year dataset: Overshooting Top Detection with SEVIRI," *Q.J.R. Meteorol. Soc.*, vol. 141, no. 688, pp. 909–915, Apr. 2015, doi: 10.1002/qj.2410.
- [12] H. J. Punge, K. M. Bedka, M. Kunz, and A. Werner, "A new physically based stochastic event catalog for hail in Europe," *Nat Hazards*, vol. 73, no. 3, pp. 1625–1645, Sep. 2014, doi: 10.1007/s11069-014-1161-0.
- [13] W. Thiery, E. L. Davin, S. I. Seneviratne, K. Bedka, S. Lhermitte, and N. P. M. van Lipzig, "Hazardous thunderstorm intensification over Lake Victoria," *Nat Commun*, vol. 7, no. 1, p. 12786, Nov. 2016, doi: 10.1038/ncomms12786.

- [14] W. Thiery *et al.*, "Early warnings of hazardous thunderstorms over Lake Victoria," *Environ. Res. Lett.*, vol. 12, no. 7, p. 074012, Jul. 2017, doi: 10.1088/1748-9326/aa7521.
- [15] K. M. Bedka, J. T. Allen, H. J. Punge, M. Kunz, and D. Simanovic, "A Long-Term Overshooting Convective Cloud-Top Detection Database over Australia Derived from MTSAT Japanese Advanced Meteorological Imager Observations," *Journal of Applied Meteorology and Climatology*, vol. 57, no. 4, pp. 937–951, Apr. 2018, doi: 10.1175/JAMC-D-17-0056.1.
- [16] M. S. P. S. A. Besari, "Deteksi Overshooting Top Menggunakan Satelit Himawari-8 di Wilayah Jabodetabek (September–November 2017)," Sekolah Tinggi Meteorologi Klimatologi dan Geofisika, Tangerang Selatan, 2018.
- [17] A. D. Vahada, "Identifikasi Overshooting Cloud Top Pada Awan Cumulonimbus di Wilayah Tropis Menggunakan Satelit Himawari-8," presented at the Seminar Nasional "Mitigasi Dan Strategi Adaptasi Dampak Perubahan Iklim Di Indonesia", Riau, Indonesia: Universitas Islam Riau, 2017, pp. 26–32. [Online]. Available: http://registrasi.seminar.uir.ac.id/prosidin_g/sem_nas17/file/SCI01706_Adinda%20Dara%20Vahada.pdf
- [18] F. S. Ariwibowo, A. A. K. Nur, and Indra, "Identifikasi Fenomena Hujan Es Berbasis Analisis Faktor Cuaca Menggunakan Citra Satelit Himawari-8 dan Data Upper Air Sounding (Studi Kasus: Kejadian Hujan Es Tanggal 20 Maret 2018 di Depok)," *jiif*, vol. 2, no. 2, Nov. 2018, doi: 10.24198/jiif.v2i2.19729.
- [19] J. A. I. Paski, D. S. Permana, A. Sepriando, and D. A. S. Pertiwi, "Analisis Dinamika Atmosfer Kejadian Hujan Es Memanfaatkan Citra Radar dan Satelit Himawari-8 (Studi Kasus: Tanggal 3 Mei 2017 di Kota Bandung)," presented at the Seminar Nasional Penginderaan Jauh ke-4, Depok, Indonesia: LAPAN, 2017, pp. 371–381.
- [20] BMKG, "Regulation of the Head of the Agency for Meteorology, Climatology and Geophysics regarding provision and dissemination of extreme weather early warnings No. 9 2022." Agency for Meteorology, Climatology and Geophysics of Republic of Indonesia, September 08th, 2022. [Online]. Available: <https://jdih.bmkg.go.id/dokumen/view?id=4197>
- [21] BMKG, "Regulation of the Head of the Agency for Meteorology, Climatology and Geophysics No. Kep.009 of 2010 concerning Standard Operational Procedures for Implementing Early Warning Reporting and Dissemination of Extreme Weather." Agency for Meteorology, Climatology and Geophysics of Republic of Indonesia, October 10th, 2010. [Online]. Available: <https://jdih.bmkg.go.id/dokumen/view?id=4157>
- [22] K. Bessho *et al.*, "An Introduction to Himawari-8/9—Japan's New-Generation Geostationary Meteorological Satellites," *Journal of the Meteorological Society of Japan*, vol. 94, no. 2, pp. 151–183, 2016, doi: 10.2151/jmsj.2016-009.
- [23] K. M. Bedka and K. Khlopenkov, "A Probabilistic Multispectral Pattern Recognition Method for Detection of Overshooting Cloud Tops Using Passive Satellite Imager Observations," *Journal of Applied Meteorology and Climatology*, vol. 55, no. 9, pp. 1983–2005, Sep. 2016, doi: 10.1175/JAMC-D-15-0249.1.
- [24] M. Kim, J. Im, H. Park, S. Park, M.-I. Lee, and M.-H. Ahn, "Detection of Tropical Overshooting Cloud Tops Using Himawari-8 Imagery," *Remote Sensing*, vol. 9, no. 7, p. 685, Jul. 2017, doi: 10.3390/rs9070685.
- [25] EUMeTrain, "Sandwich products," 2019. <https://resources.eumetrain.org/data/5/507/index.htm> (accessed October 01st, 2022).
- [26] H. J. Punge, K. M. Bedka, M. Kunz, and A. Reinbold, "Hail frequency estimation across Europe based on a combination of overshooting top detections and the ERA-INTERIM reanalysis," *Atmospheric Research*, vol. 198, pp. 34–43, Dec. 2017, doi: 10.1016/j.atmosres.2017.07.025.
- [27] M. D. Yamanaka, "Physical climatology of Indonesian maritime continent: An outline to comprehend observational studies," *Atmospheric Research*, vol. 178–179, pp. 231–259, Sep. 2016, doi: 10.1016/j.atmosres.2016.03.017.
- [28] K. M. Bedka, C. Wang, R. Rogers, L. D. Carey, W. Feltz, and J. Kanak, "Examining Deep Convective Cloud Evolution Using Total Lightning, WSR-88D, and GOES-14 Super Rapid Scan Datasets*," *Weather and Forecasting*, vol. 30, no. 3, pp. 571–590, Jun. 2015, doi: 10.1175/WAF-D-14-00062.1.
- [29] D. L. Solomon, K. P. Bowman, and C. R. Homeyer, "Tropopause-Penetrating Convection from Three-Dimensional Gridded NEXRAD Data," *Journal of*

- Applied Meteorology and Climatology*, vol. 55, no. 2, pp. 465–478, Feb. 2016, doi: 10.1175/JAMC-D-15-0190.1.
- [30] T. T. Fujita, “Overshooting thunderheads observed from ATS and Learjet,” 1974.
- [31] M. Setvák *et al.*, “A-Train observations of deep convective storm tops,” *Atmospheric Research*, vol. 123, pp. 229–248, Apr. 2013, doi: 10.1016/j.atmosres.2012.06.020.
- [32] M. Elliott, D. MacGorman, T. Schuur, and P. Heinselman, “An analysis of overshooting top lightning mapping array signatures in supercell thunderstorms,” presented at the 22nd International Lightning Detection Conference, Broomfield, Colorado, USA.